

Structural characteristics of the Lake Van Basin, eastern Turkey, from high-resolution seismic reflection profiles and multibeam echosounder data: geologic and tectonic implications

Deniz Cukur^{1,2} · Sebastian Krastel² · Yama Tomonaga^{3,4} · Hans-Ulrich Schmincke⁵ · Mari Sumita⁵ · Ayşegül Feray Meydan⁶ · M. Namık Çağatay⁷ · Mustafa Toker⁸ · Seong-Pil Kim¹ · Gee-Soo Kong¹ · Senay Horozal¹

Received: 28 November 2015 / Accepted: 24 February 2016 / Published online: 11 March 2016
© Springer-Verlag Berlin Heidelberg 2016

Abstract The structural evolution of Lake Van Basin, eastern Turkey, was reconstructed based on seismic reflection profiles through the sedimentary fill as well as from newly acquired multibeam echosounder data. The major sub-basins (Tatvan Basin and Northern Basin) of Lake Van, bound by NE-trending faults with normal components, formed during the past ~600 ka probably due to extensional tectonics resulting from lithospheric thinning and mantle upwelling related to the westward escape of Anatolia. Rapid extension and subsidence during early lake formation led to the opening of the two sub-basins. Two major, still active volcanoes (Nemrut and Süphan) grew close to the lake basins approximately synchronously, their explosive

deposits making up >20 % of the drilled upper 220 m of the ca. 550-m-thick sedimentary fill. During basin development, extension and subsidence alternated with compressional periods, particularly between ~340 and 290 ka and sometime before ~14 ka, when normal fault movements reversed and gentle anticlines formed as a result of inversion. The ~14 ka event was accompanied by widespread uplift and erosion along the northeastern margin of the lake, and substantial erosion took place on the crests of the folds. A series of closely spaced eruptions of Süphan volcano occurred synchronously suggesting a causal relationship. Compression is still prevalent inside and around Lake Van as evidenced by recent faults offsetting the lake floor and by recent devastating earthquakes along their onshore continuations. New, high-resolution bathymetry data from Lake Van reveal the morphology of the Northern Ridge and provide strong evidence for ongoing transpression on a dextral strike-slip fault as documented by the occurrence of several pop-up structures along the ridge.

Keywords Lake Van · Seismic data · Multibeam echosounder · Tectonic activity · Volcanism · Compression · Extension

✉ Deniz Cukur
dcukur@kigam.re.kr

- ¹ Petroleum and Marine Research Division, Korea Institute of Geoscience and Mineral Resources (KIGAM), 124 Gwahang-no, Yuseong-gu, Daejeon 305-350, Korea
- ² Institute of Geosciences, Kiel University, Otto-Hahn-Platz 1, 24118 Kiel, Germany
- ³ Atmosphere and Ocean Research Institute, The University of Tokyo, 5-1-5 Kashiwanoha, Kashiwa-shi, Chiba 277-8564, Japan
- ⁴ Department of Water Resources and Drinking Water, Eawag, Swiss Federal Institute of Aquatic Science and Technology, Ueberlandstrasse 133, 8600 Dübendorf, Switzerland
- ⁵ GEOMAR Helmholtz Centre for Ocean Research Kiel, Wischhofstr. 1-3, 24148 Kiel, Germany
- ⁶ Department of Geological Engineering, Van Yüzüncü Yıl University, Van, Turkey
- ⁷ Department of Geological Engineering, Istanbul Technical University, EMCOL, 34469 Maslak, Istanbul, Turkey
- ⁸ Department of Geophysical Engineering, Van Yüzüncü Yıl University, Van, Turkey

Introduction

Lake Van is situated on the high plateaus of eastern Anatolia, Turkey, at an altitude of approximately 1650 m a.s.l. (a.s.l.: above the sea level; Fig. 1). The total water volume of Lake Van is ca. 600 km³, and the present-day maximum water depth is 450 m (Degens et al. 1984; Cukur et al. 2013). Süphan volcano on its northern shore rises to an elevation of 4434 m a.s.l. (Fig. 1), the adjacent Nemrut volcano on the western shore to 3050 m a.s.l. (Fig. 1). Two

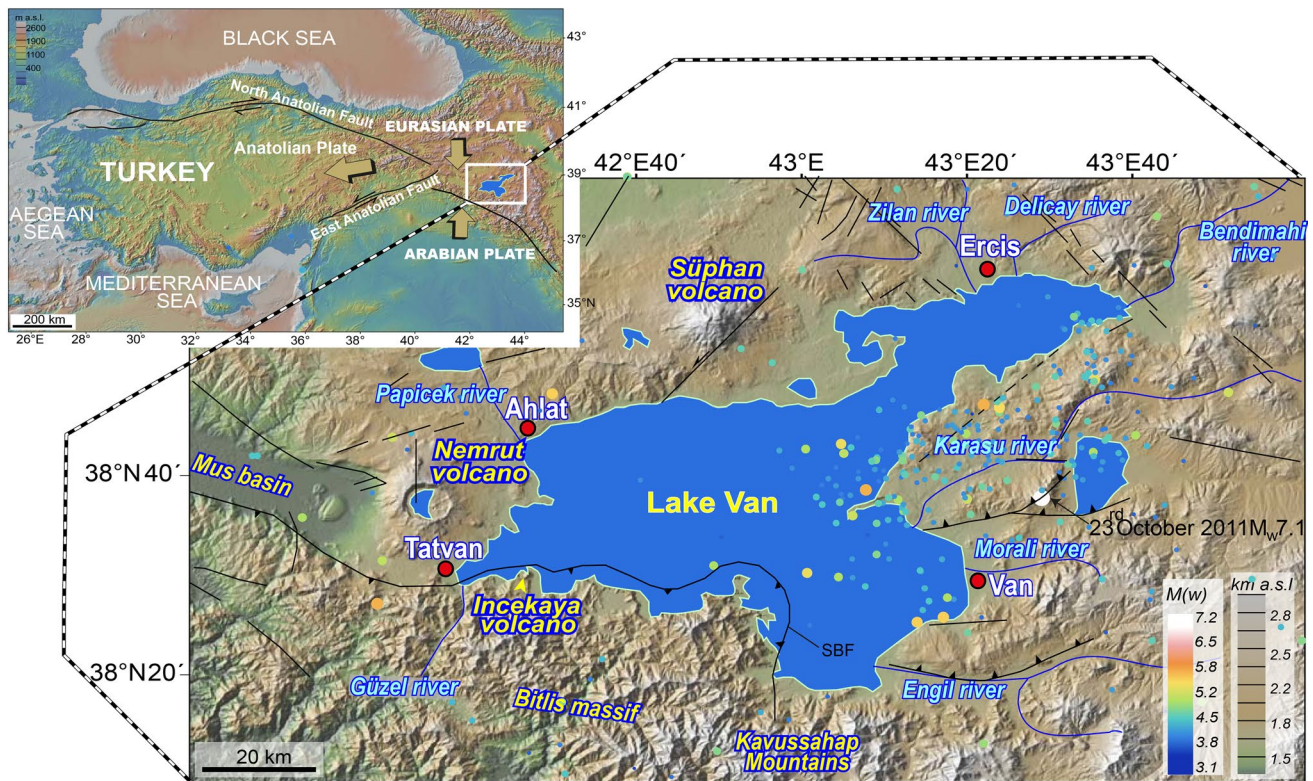


Fig. 1 Location of Lake Van and surrounding tectonic elements. Major cities are indicated by red dots. Earthquake epicenters in the Lake Van region since 1900 ($3 \leq M_w \leq 7$) are denoted by colored

dots. The earthquake data were taken from www.deprem.gov.tr. SBF South Boundary Fault

sites successfully drilled in the Northern Basin (NB) and at Ahlat Ridge (AR) in 2010 (Fig. 2; Stockhecke et al. 2014) in the framework of the ICDP (International Continental Scientific Drilling Program) show that Lake Van is an excellent Quaternary high-resolution paleoclimate archive for the Near East (Litt and Anselmetti 2014; Stockhecke et al. 2014).

Several large historic and modern earthquakes have characterized the Lake Van area (Utkucu 2013). The most recent $M_w 7.1$ earthquake on October 23, 2011, (Fig. 1) struck the eastern part of the lake near the town of Van, caused over 600 deaths and led to major economic losses (Erdik et al. 2012; Taskin et al. 2013). This earthquake drew much attention to the Lake Van area not only for being the largest seismic event of the last 100 years, but also for being one of the largest historic shocks in Turkey (Koçyiğit 2013). Several studies (Elliot et al. 2013; Fielding et al. 2013; Bayrak et al. 2013; Dogan and Karakas 2013; Toker 2013) suggest that the 2011 $M_w 7.1$ earthquake of 2011 occurred on a northward dipping reverse fault with a minor strike-slip component. All of these studies focused, however, on onshore evidence. Because Lake Van has been characterized by continuous sedimentation over at

least 600 ka (Stockhecke et al. 2014), any tectonic movement within or around the lake is likely to be recorded in the sediments. Here, we identify the main structural features within Lake Van Basin by analyzing recently acquired over 1500 km of multi-channel seismic reflection profiles in conjunction with multibeam echosounder data. These structural features provide important constraints on the evolution of Lake Van Basin and the adjacent areas. Furthermore, the imaging of pop-up structures may provide an excellent natural example of transpressional settings that can be compared with existing analog models.

Geological and physiographic setting

Lake Van, the largest and deepest lake in Turkey, lies along the collision zone between the Arabian and the Eurasian Plates (Fig. 1). The N-S convergence between these plates is estimated to be about 16 mm/year based on global positioning system measurements (Reilinger et al. 2006) and is thought to have started at ca. 13 Ma (Şengör et al. 2003). As a result of this collision, a large continental block (the Anatolian Plate) escaped in a westerly direction along the

North Anatolian and the East Anatolian fault zones (Fig. 1). The initiation of these major faults dates back to the late Pliocene (Gürbüz and Gürer 2008).

The geologic history of the basins in eastern Anatolia was also controlled, or at least influenced, by the interaction of the Arabian, Anatolian and the Eurasian Plates. However, it is still not known precisely how basin development was related to the interaction of these plates. A recent study, on the basis of geomorphic analyses of digital elevation model images, suggests that the tectonic evolution of the basins in eastern Anatolia has been controlled by lithospheric thinning and mantle upwelling related to gravity-controlled escape of Anatolia (Dhont and Chorowicz 2006). The interaction of these plates is manifested in the Lake Van region by the occurrence of several strike-slip and reverse faults (Fig. 1), intense volcanic activity and normal fault-controlled extensional basins (i.e., Mus Basin, Fig. 1; Dhont and Chorowicz 2006; Schmincke et al. 2014). The tectonic activity is still ongoing in the region as evidenced by the occurrence of several earthquakes during the past 100 years (Fig. 1).

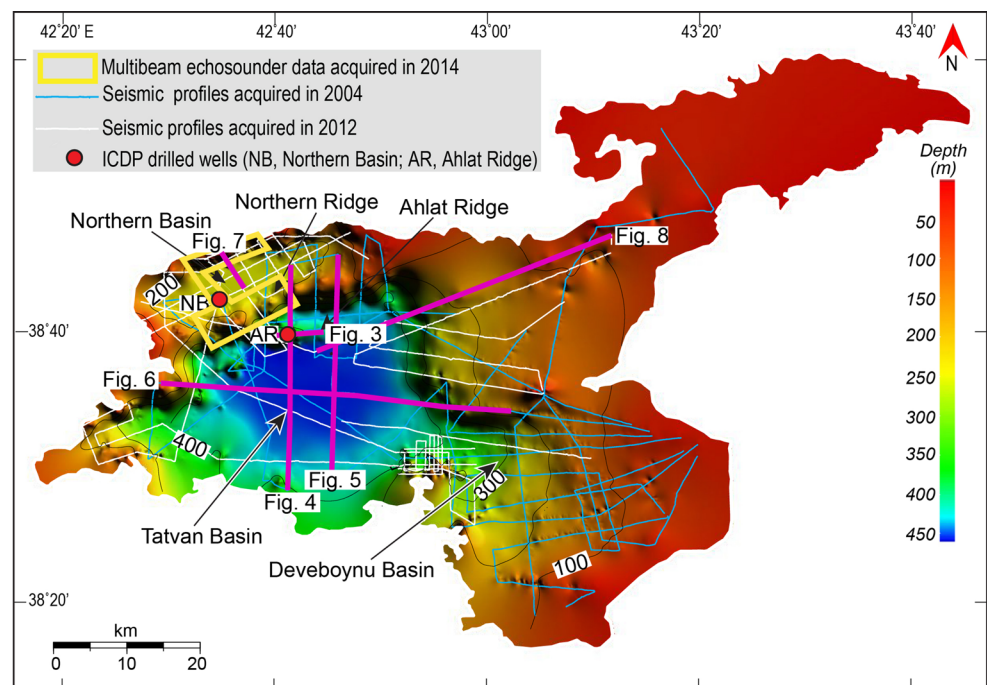
The surface area of Lake Van is approximately 3500 km² with a WSW-ENE length of about 130 km. The catchment area covers ~16,000 km² (Kempe et al. 1978) and extends far to the eastern Mus Basin. The highest elevation of the catchment area, the Bitlis massif, underlain by Paleozoic metamorphic rocks, extends south of the southern boundary of the lake, reaching 3500 m a.s.l. in elevation (Fig. 1). Volcanic rocks cover extensive areas, especially to the north and west of Lake Van (Wong and Finckh 1978; Litt et al. 2009; Sumita and Schmincke 2013; Görür et al. 2015). Eocene-to-Pleistocene clastic sediments and Upper

Cretaceous carbonates crop out east of the lake (Wong and Finckh 1978; Görür et al. 2015).

The cause and exact timing of the formation of Lake Van are unknown. Previously, it was suggested that the eruption of a lava flow from the Nemrut volcano built a dam across the Mus Basin, cutting off the drainage to ancient Murat River (Lahn 1948; Degens et al. 1984). Sumita and Schmincke (2013) suggested that Nemrut volcano grew in the hinge area between the Van Basin and the Mus Basin. Thick ignimbrites underlying the high plateau south of Tatvan may have contributed to closing of the outlet of an ancient river. Following the separation from the Mus Basin, continued subsidence and extension further fostered the formation of a large drainage basin sometime prior to ca 600 ka (Schmincke et al. 2014; Cukur et al. 2014a).

The morphology of the lake basin has been determined by seismic profiles (Cukur et al. 2013). The lake is divided into three deep sub-basins (the Northern, Tatvan and Deveboynu Basins) separated from each other by basement ridges (e.g., the Northern Ridge; Fig. 2). The deep Tatvan Basin is approximately outlined by the 400 m bathymetric contour and is separated from the smaller Ahlat sub-basin by the Ahlat Ridge (Fig. 2). The Tatvan Basin measures between 23 and 28 km and covers an area of ~400 km². The much smaller Northern Basin, covering an area of ~90 km², with a mean water depth of ~240 m is separated from the Tatvan Basin by the NE-trending Northern Ridge that is about 30 km long, ~5 km wide and rises ~300 m above the lake floor of the Tatvan Basin. The small Deveboynu Basin has an E-W length of 8 km and a N-S length of 10 km with an average water depth of 300 m.

Fig. 2 Bathymetric map of Lake Van showing the distribution of seismic reflection profiles and the location of the ICDP wells drilled at Northern Basin (NB) and at Ahlat Ridge (AR). The map also shows sub-basins of the Lake Van. *Thick purple lines* and respective figure numbers indicate the position of the seismic profiles shown in Figs. 3, 4, 5, 6, 7 and 8



Today, the lake is hydrologically closed. Major tributaries entering the lake include the Karasu, Morali and Engil rivers near the city of Van; the Guzel river near Tatvan; the Zilan, Delicay and Bendimahi rivers near Erçis; and the Papicek river near Ahlat. More than 50 % of the annual discharge is provided by the Zilan, Bendimahi and Engil rivers (Reimer et al. 2008). Since its formation, the lake has undergone dramatic fluctuations in lake level during the last ~600 ka in relation to major climatic changes (Landmann et al. 1996; Reimer et al. 2008; Kuzucuoglu et al. 2010; Cukur et al. 2014b; Tomonaga et al. 2014). The sensitivity of Lake Van to most recent changes in the hydrological regime of the surrounding region has been shown by limnological studies (Kipfer et al. 1994; Kaden et al. 2010; Tomonaga et al. 2011).

Data sets and methods

Our data comprise more than 1500 km of migrated high-resolution 2D seismic reflection profiles, multibeam echosounder data and ages from the ICDP drill site at Ahlat Ridge encompassing a depth range of about 220 m below the lake floor (Stockhecke et al. 2014; Fig. 2). The multi-channel seismic reflection datasets were collected in 2004 and 2012 with similar acquisition systems. A 16-channel (100-m-long) analog streamer was used in 2004 and a 48-channel (100-m-long) digital streamer in 2012. A Mini-GI-Gun with a frequency of 80–500 Hz was used for both surveys; these frequencies resulted in a vertical resolution of a few meters. Data processing included editing of bad traces, geometry setup, binning, velocity analysis, normal moveout (NMO) correction and stacking. The bin distance was 10 and 3 m for the 2004 and 2012 data, respectively. Acoustic and density logs from the Ahlat Ridge well were used to generate synthetic seismograms for a seismic-to-well tie that allowed to obtain time–depth relationships at the drill locations. The IHS Kingdom Suite (version 8.5) software was used to generate synthetic seismograms and to interpret and map the seismic data.

The multibeam echosounder data were collected in June 2014 with an ELAC Seabeam 1050 multibeam system (Fig. 2). We used 50 kHz transducers for this campaign, which have a designated working depth down to 2000 m. Post-acquisition data processing was performed using a MB system. The processed data were then loaded into Global Mapper software for interpretation.

Results

Seismic stratigraphy

The detailed seismic stratigraphy of Lake Van has been studied by continuous seismic profiling to about 600 m

depth (Cukur et al. 2014a). In total, 19 seismic unit boundaries (SUB) or unconformities were identified, including the top of the acoustic basement (Fig. 3). Approximate $^{40}\text{Ar}/^{39}\text{Ar}$ ages of these unconformities, based on unpublished ages and comparison with dated massive ignimbrites on land (Sumita and Schmincke 2013), were taken directly from Cukur et al. (2014a). Sequences bound by these unconformities are, from oldest to youngest, referred to as SU1–SU19. The seismic reflection profiles show that the Tatvan Basin is characterized by alternating well-stratified and chaotic seismic reflections. The well-stratified seismic facies are interpreted to be the result of undisturbed lacustrine sediments interbedded with turbidites and tephra layers (Cukur et al. 2014a). The chaotic seismic facies are interpreted as large mass-transport deposits that resulted from tectonic and volcanic activity along the lake margins (Fig. 3; Cukur et al. 2014a). The Northern Basin was filled predominantly by mass-flow deposits sourced in the highlands along the northwestern basin margin possibly triggered by ongoing tectonic activity. On the morphologically elevated ridges, such as Ahlat ridge that was drilled, lacustrine sediments and tephra layers predominate (Fig. 3; Cukur et al. 2014a). Prograding clinoforms (deltaic deposits), which had formed by lake-level fluctuations (Cukur et al. 2014b), cover most of the shelf and slope areas. Hence, the sedimentary infill in the sub-basins was primarily controlled by climatic, tectonic and volcanic processes. Lake Van appears to have responded drastically to climatic changes as suggested by numerous lake-level fluctuations (Cukur et al. 2014b). We thus interpret that climate change had a significant impact on the sedimentary history of the lake.

Structural analysis of seismic reflection profiles

Seismic profile 1 (SP1; Fig. 4) is about ~29 km long and trends N–S, traversing the Tatvan Basin, Ahlat Ridge, Ahlat sub-basin, Northern Ridge and the Northern Basin. The northern part of the Tatvan Basin is cut by a large normal fault, while the southern part of the basin is bound by a reverse fault (South Boundary Fault, SBF; Cukur et al. 2013). Sediment strata, abutting against the SBF scarps, are tilted upward. Thinning of sedimentary layers against the fault is also evident. SP1 shows the Ahlat Ridge bound by steep reverse faults. The acoustic basement and the overlying sedimentary units appear to be folded and faulted. The ridge dies out and inversion disappears to the east (Fig. 5a). The Northern Ridge that separates the Tatvan and Northern Basins is a prominent NE-trending ridge that rises up to ~300 m above the lake floor of the Tatvan Basin. The southern and northern flanks of the ridge are cut by large faults; the fault on its southern flank has a vertical displacement of ~500 m. The ridge is draped by a 20-m-thick

Fig. 3 Seismic unit boundaries (in total 19, from SUB1 to SUB19), including the top of the acoustic basement (after Cukur et al. 2014a). Sequences bounded by these boundaries are referred to as SU1 to SU19 from oldest to youngest. The vertical black line at Ahlat Ridge indicates the position of the ICDP PaleoVan drill site where 220-m-long sedimentary sequence has been recovered (Stockhecke et al. 2014). An alternating succession of well-stratified and chaotically reflecting layers characterizes the basin sediments. The well-stratified reflections, on the basis of drilled cores, are interpreted as undisturbed lacustrine sediments interbedded with tephra layers and distal turbidites (Cukur et al. 2014a). The chaotic layers represent mass-transport deposits (MTDs) formed by tectonic and volcanic activity (Cukur et al. 2014a)

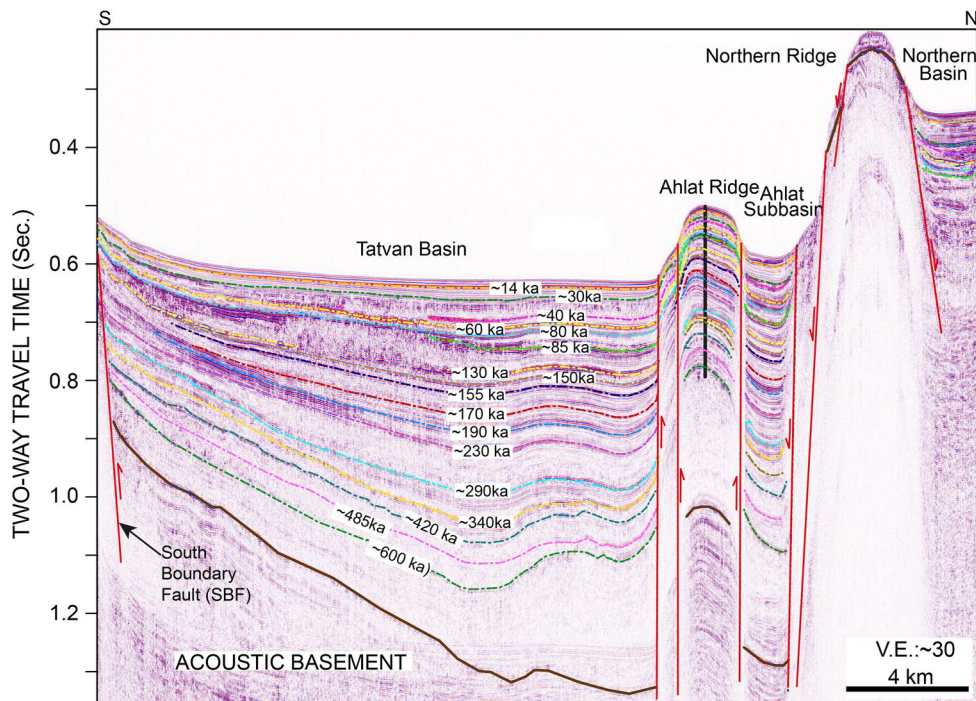
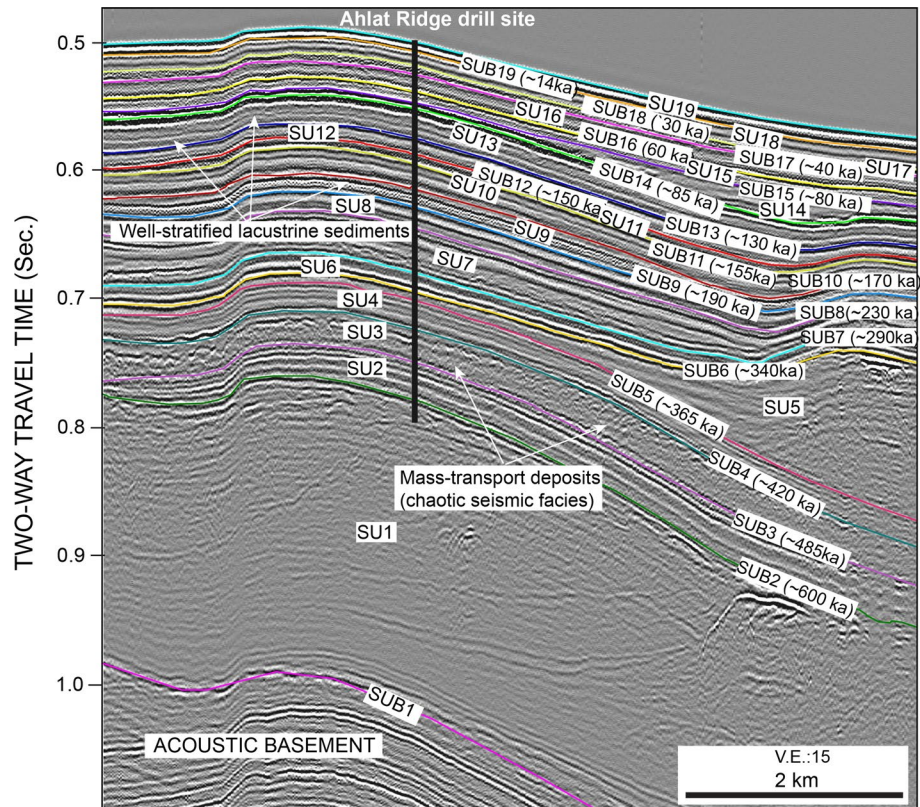
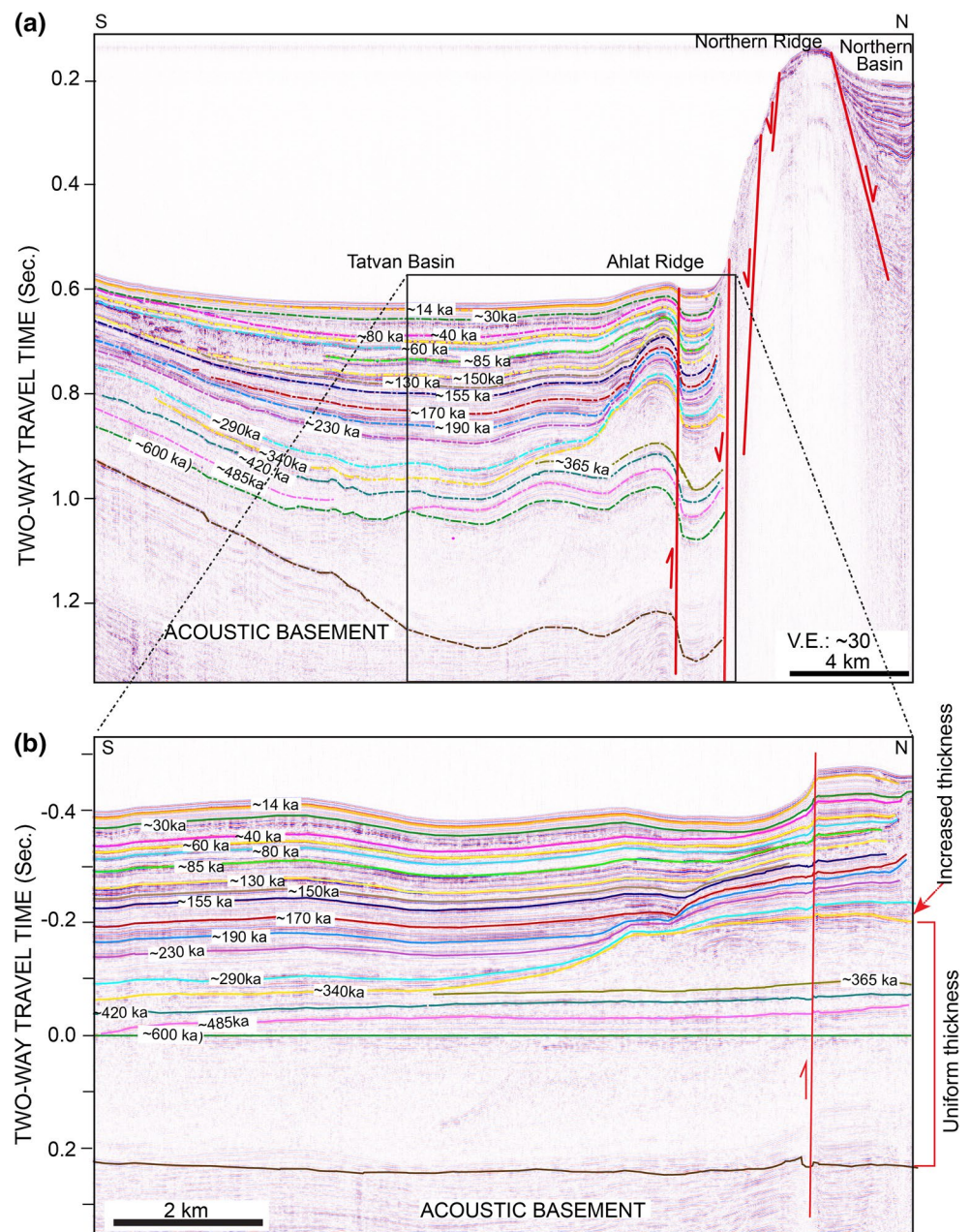


Fig. 4 Seismic profile 1 (SP1) traversing the Tatvan Basin, Ahlat Ridge, Ahlat sub-basin, Northern Ridge and the Northern Basin. The southern part of the Tatvan Basin is cut by a reverse fault (named as South Boundary Fault, SBF), while the northern part is offset by a large normal fault. The sedimentary layers become thinner and appear to be tilted toward the SBF. The EW-trending Ahlat Ridge is bound

by steep reverse faults; the sediments over the ridge, including the acoustic basement, are folded and uplifted. The Northern Ridge is flanked by two large faults. The vertical black line at Ahlat Ridge indicates the position of the ICDP PaleoVan well. See Fig. 2 for the exact location of SP1

Fig. 5 **a** Seismic profile 2 (SP2) is extending from southern margin of the lake to the Northern Basin. SP2 shows that Ahlat Ridge structure forms a broad anticline; the crest of the Ahlat Ridge is less exposed at the lake floor. The Northern Ridge appears to have disrupted by numerous faults. **b** Flattened seismic section along ~600 ka boundary. The sequences below ~340 ka boundary do not exhibit changes in thickness along the fault plane, whereas the seismic unit above ~340 ka boundary thickens rapidly. This indicates that Ahlat Ridge started to form between ~340 and ~290 ka. See Fig. 2 for the exact location of SP2



sedimentary cover and largely lacks internal reflectors suggesting an igneous origin.

Seismic profile 2 (SP2) is about 30 km long and parallels SP1, located approximately 5 km to the east (Fig. 5a). This profile clearly delineates a steeply dipping reverse fault that bounds the Ahlat Ridge. This fault offsets both the acoustic basement and the overlying seismic units; vertical displacement of the fault reaches up to 80 m at the acoustic basement and decreases to <10 m at the seafloor. Here, the elevation of the ridge appears to have decreased (~10 m) compared to that of SP1 which is about 100 m. The Northern Ridge shows an irregular surface largely due to pervasive deformation of near-vertical faults that

continue into the basement. Acoustically, the ridge is characterized by disorganized reflections without any coherent internal reflection (i.e., opaque reflection).

Differential thickening and thinning onto sedimentary structures can be potentially used to constrain their growth through time. For this purpose, a part of profile SP2 is flattened along a ~600 ka boundary in Fig. 5b. Here, the initial movement of Ahlat Ridge structure is indicated by abrupt change in thickness of seismic units above the 340 ka boundary across the fault plane. The underlying seismic units show uniform sediment thicknesses on both sides of the fault plane, suggesting that Ahlat Ridge did not exist at the time of their deposition. If the ridge was formed before

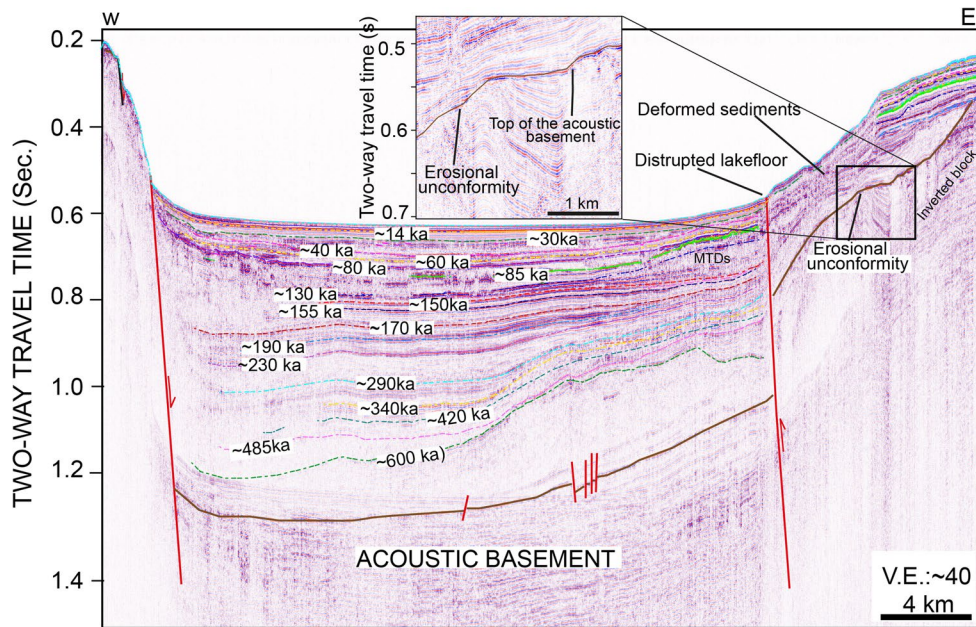


Fig. 6 Seismic profile 3 (SP3) traversing the Tatvan Basin in an EW direction. The Tatvan Basin forms a typical half-graben structure associated with extensional tectonics. To the west, the basin is cut by a steep eastward dipping normal fault. Thickening of sediments toward the respective fault is also evident. To the east, the basin is offset by a significant reverse fault; this fault offsets the basement with a vertical displacement of ~200 m. East of the reverse fault,

the topmost part of the acoustic basement appears to form an erosional unconformity, suggesting tectonic uplift and subsequent erosion before the formation of the basin of Lake Van ~600 ka ago. The reverse fault appears to be still active today, slightly disrupting the lake floor. The tectonic activity along this fault deformed the overlying lacustrine sediments. See Fig. 2 for the exact location of SP3

deposition of these units, their thickness should not be consistent on both sides of the fault plane.

Seismic profile 3 (SP3; Fig. 6) is about 40 km long and perpendicular to SP1 and SP2. The western margin of Tatvan Basin is formed by a major NE-trending normal fault downthrown to the east. The basin sediments below ~150 ka boundary including the acoustic basement dip gently westward toward this fault. Tilting of higher sedimentary sections along the fault is also evident. Smaller extensional faults are present locally at the deep sedimentary sections of Tatvan Basin (Fig. 6), most lacking growth patterns on their flanks. In the east, in contrast, a major reverse fault appears to be active today, offsetting the lake floor (Fig. 6). Here, the top of the acoustic basement is evident as an erosional unconformity and the sediments above the fault appear to be deformed and faulted. Chaotic seismic reflections, interpreted as mass-transport deposits (Cukur et al. 2014a), are seen on the downthrown block, immediately next to the reverse fault. The reverse fault has a vertical displacement of ~200 m.

Seismic profile 4 (SP4; Fig. 7) is about 5.5 km long and trends NW-SE in the Northern Basin that is bound to the northwest by an NE-trending normal fault, characterized by an upward-steepening plane. This fault offsets the lake floor with a minimum throw of 150 m. The sedimentary units progressively thin toward the NE-bounding fault.

The shallow basement at the NW end of the seismic section appears to be offset by several small-scale normal faults.

Seismic profile 5 (SP5; Fig. 8) is about 25 km long, trends NE and traverses the northeastern part of the lake. This area appears to have undergone significant recent inversion; here, sediments, at least 40 m thick, were truncated by the SUB19 unconformity (~14 ka). The SW part of the section is cut by a large reverse fault, accompanied by smaller normal faults. The fault appears to have displaced prograding clinofolds by 40 m. The reverse fault seems to be active today, slightly cutting the lake floor. Many gentle symmetrical anticlines and synclines are also present in the NE part of the section. These structures are mainly oriented E-W, parallel to the general trend of the major stress direction. All folds observed in Lake Van are located mainly in the northern half of the lake.

Depth structure of the acoustic basement and total sediment thickness

The top of the acoustic basement (Fig. 9a) is consistently mappable only in the central part of the lake. The basement is cut by dominantly NE-trending faults (Fig. 9a), most dipping SE, but NW-dipping faults also occur. EW-trending reverse faults are present locally. The acoustic basement, shallowest (<50 m) in the east, is bound by an

Fig. 7 Seismic profile 4 (SP4) trends NW, traversing the Northern Basin. The NW part of the section is cut by a large normal fault, accompanied by smaller normal faults. Sediments thin gradually toward the normal fault. See Fig. 2 for the exact location of SP4

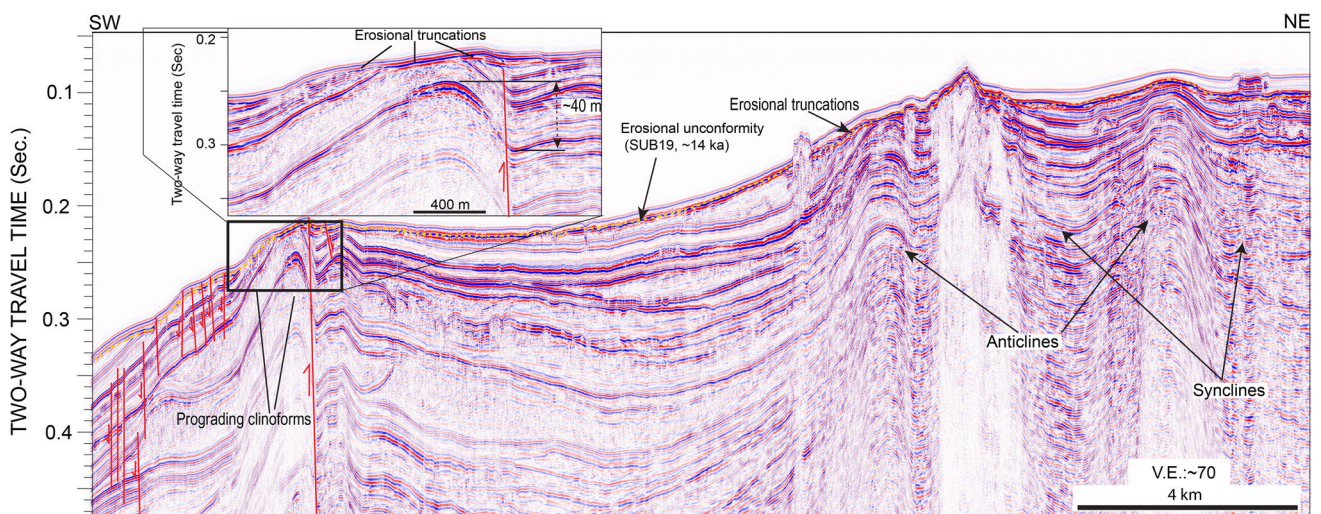
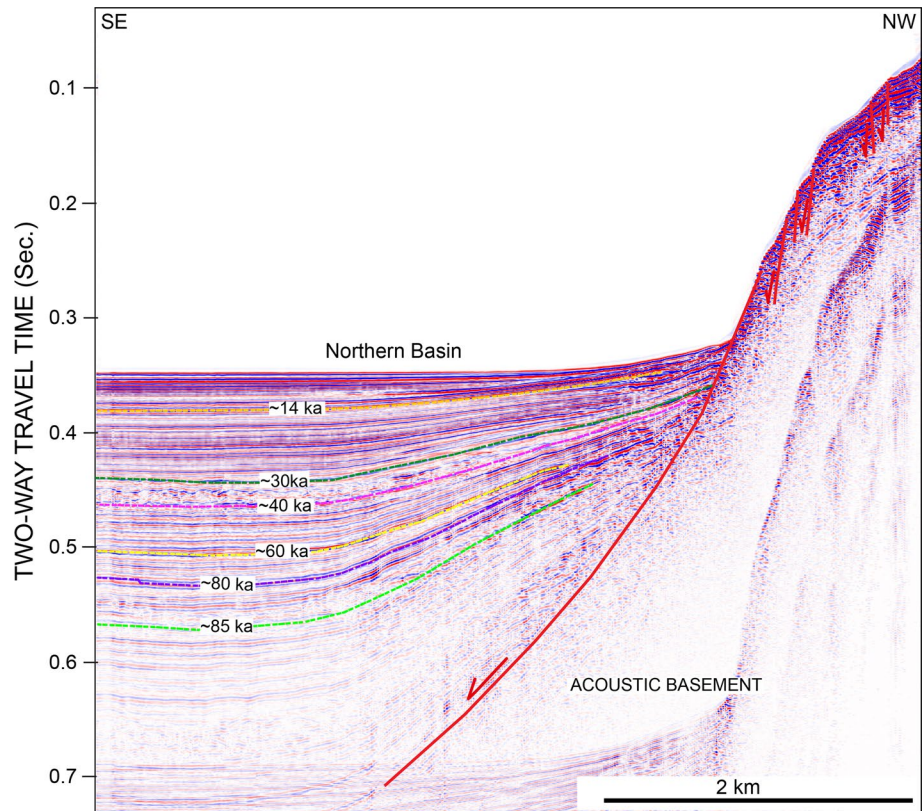


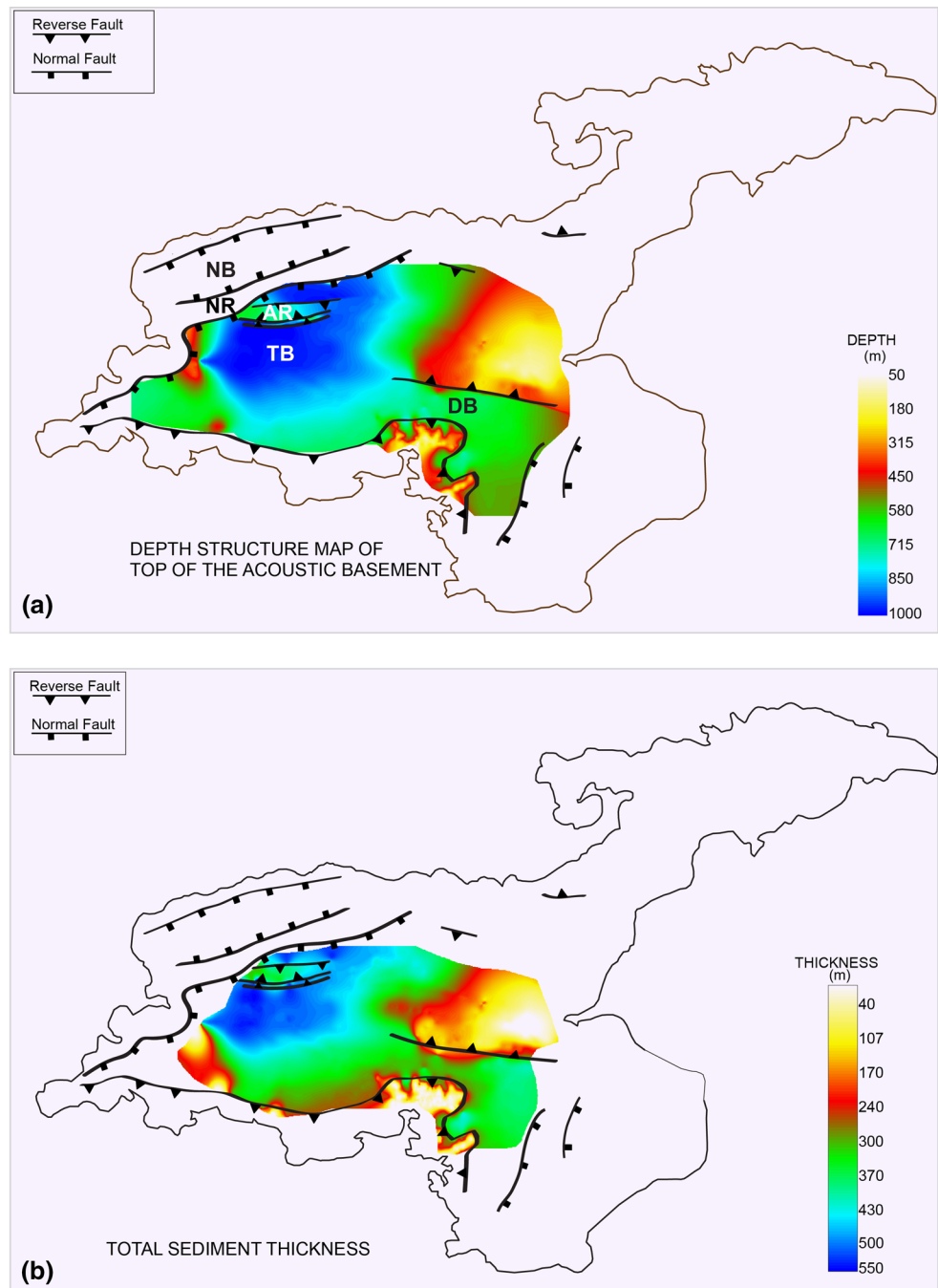
Fig. 8 Seismic profile 5 (SP5) crossing the NE corner of the lake. This part of the lake appears to have undergone recent, significant inversion; here the uppermost lake sediments were leveled by

the SUB19 unconformity (~14 ka). Several anticlinal folds are also observed. See Fig. 2 for the exact location of SP5

EW-trending reverse fault. Maximum depths of more than 850 m occur in the Tatvan Basin (TB), suggesting that maximum subsidence is located in this area. The EW-trending Ahlat Ridge in the central part of TB is also well defined. Overall, the total thickness map (Fig. 9b) shows

a pattern similar to that of the acoustic basement depth structure. The shape of the acoustic basement is, therefore, directly defined by the thickness distribution of sedimentary strata in the lake. Total sediment thickness exceeds 500 m in the TB.

Fig. 9 **a** Depth structure map of the top of the acoustic basement. The major basement faults are oriented NE, oblique to the NS-compressive stress. EW-trending reverse faults are also seen. The depths of the acoustic basement range from <50 m in the east to over 900 m in the west. *NB* Northern Basin, *NR* Northern Ridge, *AR* Ahlat Ridge, *TB* Tatvan Basin, *DB* Deveboynu Basin. **b** Overall, the map of the total thickness mirrors the basement structure, suggesting that the sedimentation in Lake Van is influenced by the morphology of its basement. The sediment thicknesses in the TB reach more than 500 m. The thinnest deposits (<100 m) are seen over the inverted block in the east

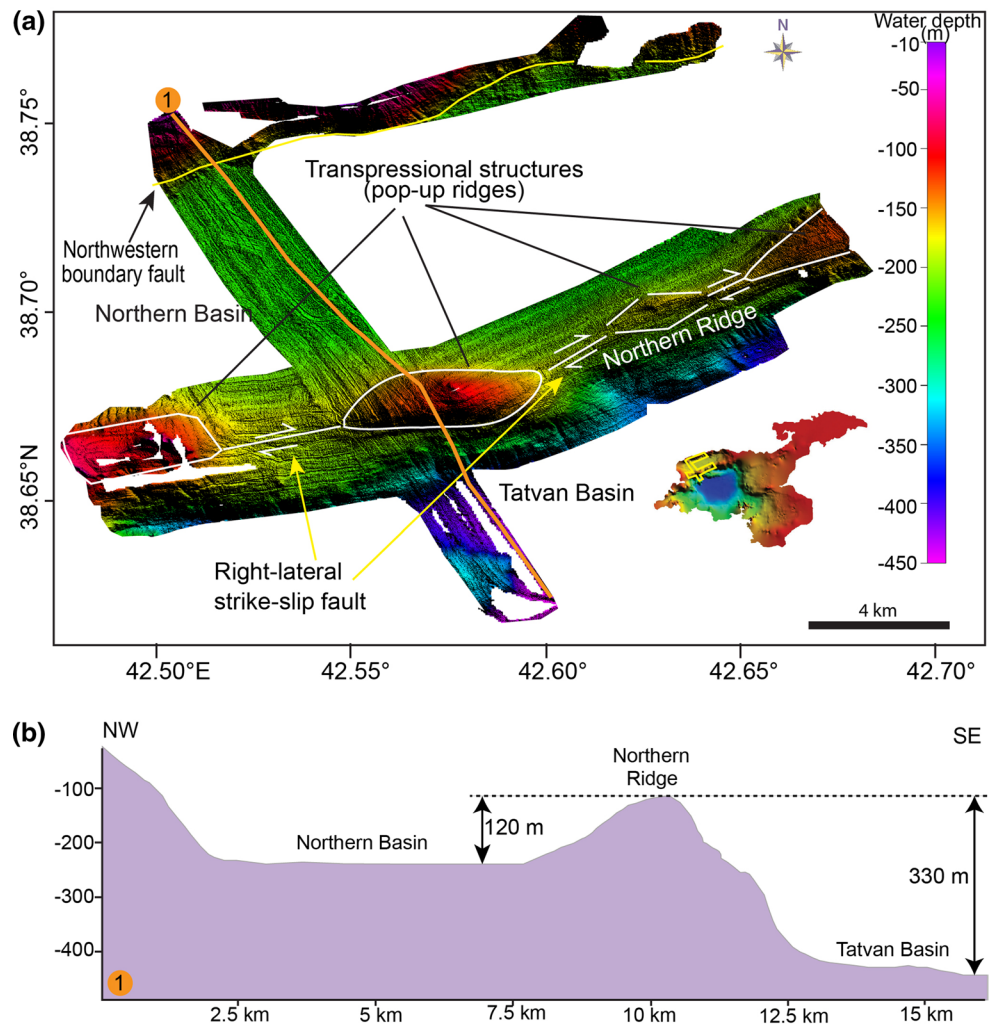


Results of multibeam echosounder data

Newly acquired multibeam data reveal the morphology and structure of the Northern Ridge (Fig. 10a) that separates the Tatvan and Northern Basins. The ridge rises up to more than 300 m above the lake floor of the Tatvan Basin, and its top is at a depth of <100 m (Fig. 10b). The bathymetric data clearly show the presence of pop-up structures

along a NE-trending right-lateral (dextral) strike-slip fault (Fig. 10a). The bathymetric data, therefore, indicate that the Northern Ridge has been experiencing transpression on strike-slip faults. These structures are very similar to features observed from dextral strike-slip analog models (Rasas et al. 2009). Additionally, the data image traces of a NE-trending fault to the northwest are described in Fig. 7 (SP4).

Fig. 10 **a** Multibeam bathymetric data from the Northern Ridge showing several transpressional structures (pop-up ridges) developed along a right-lateral strike-slip fault. *White arrows* indicate the interpreted sense of shear. **b** NW-SE oriented bathymetric profile showing the morphology of the Northern Basin, the Northern Ridge and the Tatvan Basin



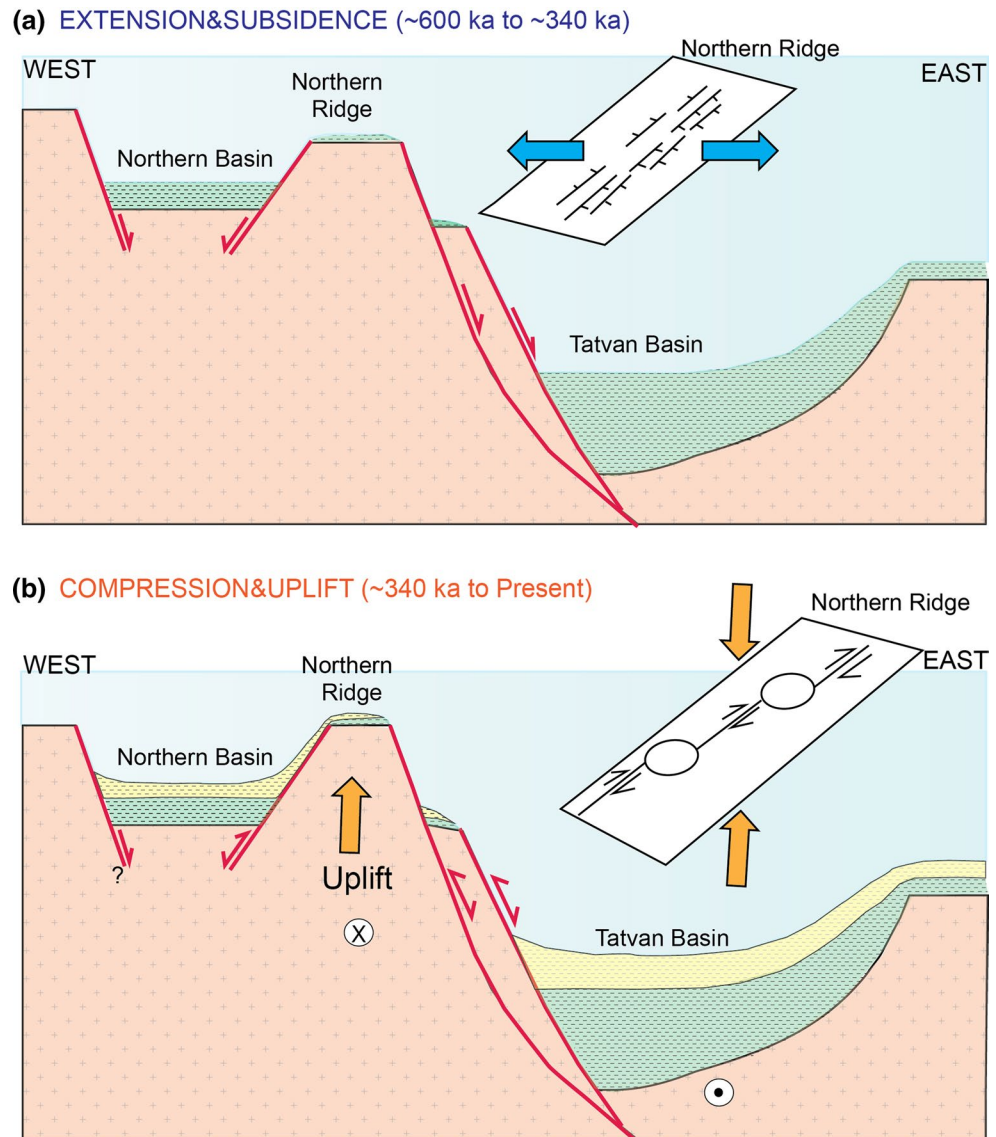
Discussion

The seismic reflection profiles show that Lake Van comprises graben and half-graben structures (up to ~550 m thick) that are bound by major NE-trending faults, oblique to the main trend of the present-day NS-directed compressional regime. The NE-trending faults further suggest E-W extension and subsidence (Fig. 11a) of the basins within Lake Van in response to a tensional regime synchronous with continental collision and convergence in eastern Turkey. The NS-compressive stress that was effective between the collision of the Arabian and Eurasian plates could easily be accommodated by extension along a strike-slip zone linking these two major systems.

Şengör and Kidd (1979) previously suggested active shortening and crustal thickening and inferred the presence of numerous thrusts in the Lake Van region. Recent studies show, however, that the lithosphere in eastern Turkey is anomalously thin (~60–80 km) consistent with an oceanic slab detachment model (Angus et al. 2006). Furthermore,

seismic refraction data for eastern Anatolia suggest a complete absence of mantle lithosphere beneath the plateau (Gök et al. 2007). Dhont and Chorowicz (2006), based on observations from digital elevation model images from eastern Anatolia, show that the orientations of the tectonic and volcanic structures fit with the tectonic regime characterized by N-S shortening and E-W lengthening. These authors further attributed this tectonic setting to mantle upwelling and crustal thinning resulting from westward escape of Anatolia perpendicular to the direction of the Arabia–Eurasia shortening. These results are also consistent with the high heat flow and copious volcanic activity across eastern Anatolia (Kempe et al. 1978). Indirect evidence for the presence of an extensional tectonic regime in this area is provided by Nemrut volcano. The magmas of Nemrut volcano are alkaline to peralkaline, which is typical for rift volcanoes (Schmincke et al. 2014; Macdonald et al. 2015). Our data do not favor a model of ongoing crustal thickening due to continental thickening, but rather support crustal thinning and mantle upwelling related to westward

Fig. 11 Schematic model illustrating the structural evolution of the basins within Lake Van. **a** Between ~600 ka BP and ~340 ka BP, extension dominated the lake basins forming the graben and half-graben depocenters. **b** From 340 ka BP onward, the extension was taken over by the compression that created transpressional structures (pop-up ridges) bound by reverse faults across the Northern Ridge. The preexisting normal faults also appear to have been reactivated as a result of the compression



escape of Anatolia as evidenced by subsidence of the Lake Van Basin as well as the dominance of extensional faulting across the lake margins. Our data suggest that Lake Van basin lies in a region characterized by synconvergent extension (Gögüs and Pysklywec 2008; see their Fig. 4).

The base of the upper 220 m of the Lake Van sediments as drilled at AR is ca. 600 ka old (Stockhecke et al. 2014), but the age and lithology of the underlying sediment fill are unknown. Lake Van started to develop some time prior to ~600 ka ago. Lahn (1948) and Degens et al. (1984) suggested that Lake Van is the product of damming of a river by a lava flow. The western part rapidly dried up and was filled with sediments. The water level rose significantly in the eastern part from the impoundment of water to form the modern lake. We favor the formation of the lake by tectonic activity, since the lake basin is almost completely bound by faults forming graben and horst topography as evidenced by our data. As

a result of this topography, a graben lake could have easily developed and subsequently been filled with freshwater and sediments. This interpretation is also supported by drill cores as the basal layers on drill site AR consist of coarser grains, shells and mollusks reflecting initial lake formation under freshwater conditions (Cukur et al. 2014a). Thus, we propose that the origin of the lake is basically due to the extensional tectonics that caused graben and half-graben structures.

The initial formation of Lake Van may have been further controlled by the growth of Nemrut Volcano before ca. 600 ka in the hinge area between Van and Mus grabens, thick ignimbrites extending from the volcano and/or the collapse of excentric domes, all processes that could have led to the formation of a major sill toward the eastern entrance to adjacent Mus basin (Sumita and Schmincke 2013; Schmincke et al. 2014). Drainage from this morphological high was thus mainly to the south.

The southern edge of the lake, bound by the Bitlis metamorphic massif, is cut by the EW-trending reverse SBF (Cukur et al. 2013). The sedimentary strata abutting against the fault scarps are dragged upward, suggesting that they predate, or are contemporaneous with, the faulting. The fact that this holds true even for the topmost layers indicates that faulting continues until today. Fourteen of the earthquakes that occurred after 1999 and for which the epicenter determinations are particularly accurate (Pinar et al. 2007) lie along the SBF and provide clear evidence that this fault is still active. Several stacked mass-transport deposits, mostly confined to the southern part of the lake, support the idea that this fault has been active throughout the evolution of the lake (Cukur et al. 2014a). The continuation of the SBF can also be traced on land (Fig. 1). There is well-documented field evidence suggesting the presence of reverse faulting along the northern margin of the Bitlis Massif, where Neogene lacustrine limestones of the Mus area are exposed 700 m lower than similar limestones found on the peaks of the Bitlis Massif to the south (Hall 1976).

The extensional regime appears to have been temporarily replaced with compressional movements at a relatively late stage in the central part of the basin (Fig. 11b). Seismic reflection data show that Ahlat Ridge might have been inverted between ~340 and 290 ka (Fig. 5b). This uplift created an accommodation space in the southern and northern parts of the Ahlat Ridge (Fig. 5a; sedimentary unit between the ~290 and ~230 ka boundaries) where the thickest sediments occurred in these areas of the lake. Today, the EW-trending Ahlat Ridge structure indicates NS compression, consistent with the GPS measurements and regional tectonic pattern suggested by Reilinger et al. (2006) for eastern Anatolia. The reverse faults that bound the ridge show little continuity in an EW direction, and the ridge dies out toward the east (Fig. 5a), possibly indicating a plunging fold. The formation of folds only in the northern part of the section (Figs. 4, 5, 8) may further suggest that faulting was controlled by local factors such as the development of transpressional faults in line with evidence observed from multibeam bathymetric data (see below).

The presence of pop-up structures at the Northern Ridge provides evidence for ongoing transpression along the NE-oriented dextral strike-slip fault (Fig. 10a). It thus seems very likely that the extension appears to have been replaced by compression along the preexisting NE-trending faults. It is, however, still unclear what caused the onset of the compressional deformation along the ridge. It might well be that the respective tectonic change in the study area is related to a change in the regional-scale plate geodynamics. As a result of plate reorganization, a number of distinct episodes of extension probably occurred in the Lake Van Basin, punctuated by compressional events that were accompanied by uplift.

Our interpretation of the seismic data suggests that a significant tectonic inversion took place in the northeastern part of the lake sometime before 14 ka (Fig. 8). This event led to the formation of several folded structures and reverse faulting in this part of the lake. Major uplift of lake sediments by several tens of meters is evident on Halepkalesi Peninsula approximately the western continuation of Ahlat Ridge (Sumita and Schmincke 2013). Folding and the accompanying uplift and erosion had ceased by 14 ka which truncates the folds (Fig. 8). SUB19 thus represents a major erosional unconformity over the lake margins with as much as 40 m of sedimentary section being removed from some anticlines in this area. The same unit boundary also represents the start of the transgression of the lake that, judging from the sediments drilled at AR, appears to have continued until the present (Cukur et al. 2014a; Stockhecke et al. 2014). This compressional event is also evidenced by several micro-deformational structures on the drill cores at AR (Schmincke et al. 2014). In addition, this event might have triggered a closely spaced swarm of several explosive bursts of Süphan volcano which occurred at the same time (Schmincke et al. 2014), seismic triggering of volcanic eruptions being common (Manga and Brodsky 2006).

Uplift and erosion took place repeatedly at the eastern margin of Lake Van along the EW-trending fault (Fig. 6), punctuated by periods of subsidence. Here, the top of the acoustic basement forms a significant erosional unconformity as evidenced by tilted and truncated underlying strata, indicating a compressional movement and subsequent erosion before the formation of Lake Van. Faulting appears to continue to the present as it offsets the current lake floor by 20 m (Fig. 6). We speculate that the EW-trending fault may be the lakeward continuation of the major fault that struck the region of Van in 2011 (Fig. 12), as both faults have the same E-W strike and the same reverse character. Also, recent microseismic monitoring around the city of Van has revealed the presence of high seismic activity along this fault (KOERI 2011). Our data indicate that this fault has been quite active for a long time, even long before the formation of the Lake Van Basins, i.e., prior to ~600 ka. Surprisingly, this major fault zone had not been recognized previously due to absence of seismic reflection profiles. Further studies such as multibeam bathymetric and sediment coring are urgently needed to improve our understanding of the nature and timing of future earthquakes in this area.

Conclusions

1. Seismic reflection data reveal major structural features including NE-trending faults bounding the Tatvan and Northern Basins of Lake Van Basin, EW-trending

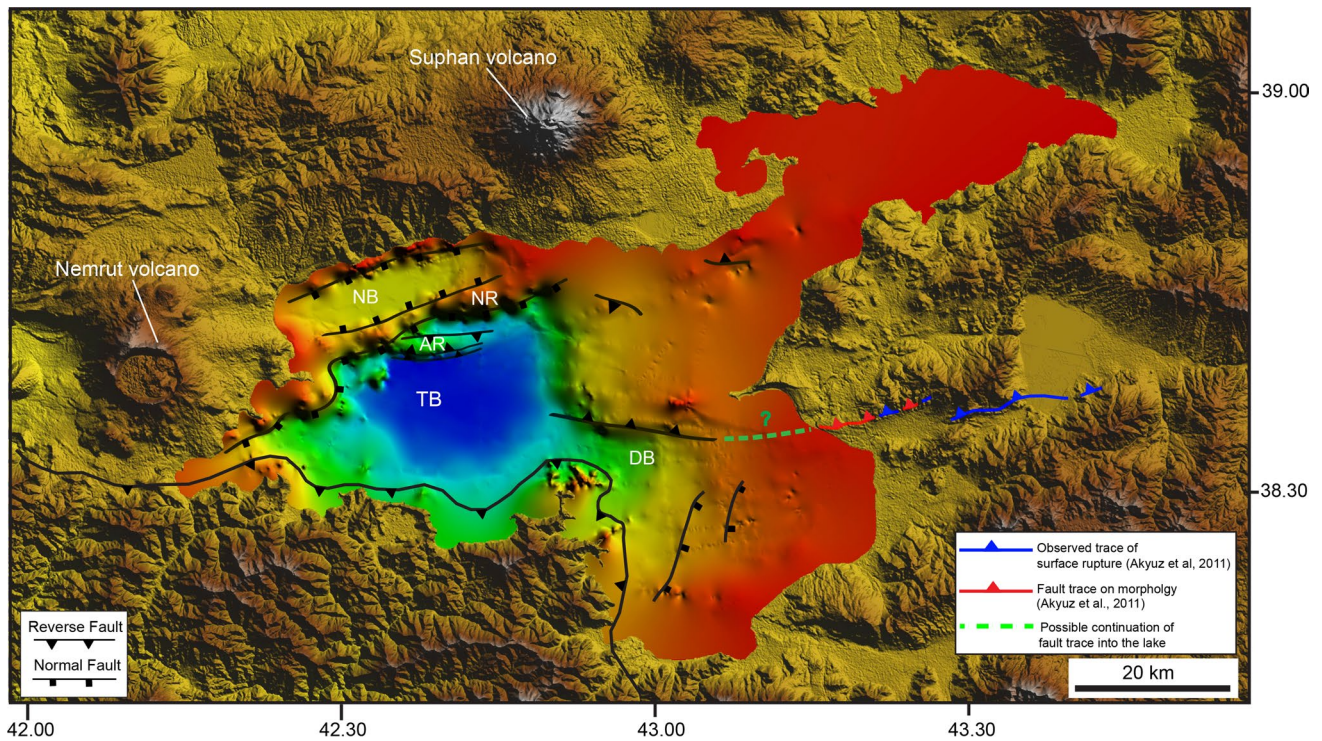


Fig. 12 Bathymetry of Lake Van superimposed with interpreted faults (*black lines*) from the seismic profiles. Observed (*red lines*) and morphological trace (*blue lines*) of source fault that ruptured during the 2011 Van earthquake (after Akyüz et al. 2011). The *dotted green*

line outlines the possible lakeward fault extension. We suggest that the EW-trending fault could represent a continuation of the reverse fault to the east, along which strong earthquake occurred

- reverse faults and numerous anticline/syncline structures in the northeastern part of the lake.
2. The NE-trending faults, graben and half-graben structures, and the gradual thickening of sediments toward the fault scarps are strongly suggestive of an extensional regime resulting from mantle upwelling and crustal thinning possibly related to the westward escape of Anatolia Plate as suggested by previous authors for eastern Anatolia. Extension was taken over by compression between ~340 and ~290 ka.
3. New, high-resolution multibeam bathymetric data reveal transpression-related structures that have formed on a northeast trending strike-slip fault (dextral shear sense) in the Northern Ridge. This further implies that the Northern Ridge has accommodated much of the N-S oriented compression throughout the lake.
4. The northeastern part of the lake experienced significant inversion prior to ~14 ka that resulted in a series of anticlines, synclines and reverse faults. This event appears to coincide with a major swarm of volcanic eruptions of Süphan volcano implying a causal relationship.
5. The EW-trending Ahlat Ridge structure began to form between ~340 and ~290 ka ago and continues today, resulting in a prominent elevation at the lake floor.

6. The eastern margin of the lake experienced multiple inversions along an EW-trending reverse fault. The tilted basement strata and the subsequent erosion over the inverted block suggest prominent inversion long before lake formation. This fault seems presently seismically active, as evidenced by the overlying deformed strata and offsetting of the lake floor, and could represent the continuation of the reverse fault to the east, along which the most recent strong earthquake occurred in 2011. Hence, the study of the sub-lacustrine part of this fault is very important for an adequate risk assessment of the area in order to develop strategies for minimizing the consequences.
7. The present study provides new insights that will support future studies and monitoring strategies related to major seismic events in the region of Lake Van.

Acknowledgments The authors acknowledge funding of the PaleoVan drilling campaign by the International Continental Scientific Drilling Program (ICDP), the Deutsche Forschungsgemeinschaft (DFG; Grants KR2222-9, KR2222/15 and SCHM 250/93-1) and the Swiss National Science Foundation (SNF Grants 20FI21_124972, 200021_124981 and 200020-143340). This work was also supported by the Marine Geological and Geophysical Mapping of the Korean Seas Project (GP2015-042) and by the Study on marine geology and mineral resource in buried paleochannel of Seonjin River, South Sea, Project (GP2015-040) for DC, GSK and SPK and the EU Seventh

Framework Programme for Research and Technological Development (Marie Curie International Outgoing Fellowship, Contract PIOF-GA-2012-332404) for YT. Senay Horozal was supported by part of the project titled ‘International Ocean Discovery Program,’ funded by the Ministry of Oceans and Fisheries, Korea (Grant: 20110183). We thank our colleagues from the Istanbul Technical University (Istanbul, Turkey) and from the Kiel University (Kiel, Germany) team for support during data collection. Special thanks go to our captains, Mete Orhan and Munip Kanan, for their untiring commitment during the seismic data acquisition.

References

- Akyüz S, Zabcı C, Sancar T (2011) 23 Ekim 2011 Van depremi hakkında ön rapor. İstanbul Teknik Üniversitesi, İstanbul (**in Turkish**)
- Angus DA, Wilson DC, Sandvol E, Ni JF (2006) Lithospheric structure of the Arabian and Eurasian collision zone in Eastern Turkey from S-wave receiver functions. *Geophys J Int* 166:1335–1346
- Bayrak Y, Yadav RBS, Kalafat D, Tsapanos TM, Çınar H, Singh AP, Yılmaz Ş, Öcal F, Koravos G (2013) Seismogenesis and earthquake triggering during the Van (Turkey) 2011 seismic sequence. *Tectonophysics* 601:163–176
- Cukur D, Krastel S, Schluter FD, Demirbag E, Imren C, Niessen F, Toker M, PaleoVan-Working Group (2013) Sedimentary evolution of Lake Van (Eastern Turkey) reconstructed from high resolution seismic investigations. *Int J Earth Sci* 102(2):571–585
- Cukur D, Krastel S, Schmincke HU, Sumita M, Cagatay N, Meydan AF, Damcı E, Stockhecke M (2014a) Seismic stratigraphy of Lake Van, eastern Turkey. *Quat Sci Rev* 104:63–84
- Cukur D, Krastel S, Schmincke HU, Sumita M, Tomonaga Y, Cagatay N (2014b) Water level changes in Lake Van, Turkey, during the past ca. 600 ka: climatic, volcanic and tectonic controls. *J Paleolimnol* 52(3):201–214
- Degens ET, Wong HK, Kempe S (1984) A geological Study of Lake Van, Eastern Turkey. *Geol Rundsch* 73(2):701–734
- Dhont D, Chorowicz J (2006) Review of the neotectonics of the Eastern Turkish-Armenian Plateau by geomorphic analysis of digital elevation model imagery. *Int J Earth Sci* 95(1):34–49
- Dogan B, Karakas A (2013) Geometry of co-seismic surface ruptures and tectonic meaning of the 23 October 2011 Mw 7.1 Van earthquake (East Anatolian Region, Turkey). *J Struct Geol* 46:99–114
- Elliott JR, Copley AC, Holley R, Scharer K, Parsons B (2013) The 2011 Mw 7.1 Van (Eastern Turkey) earthquake. *J Geophys Res Solid Earth* 118:1–19
- Erdik M, Kamer Y, Demircioglu M, Sesetyan S (2012) 23 October 2011 Van (Turkey) earthquake. *Nat Hazards* 64:651–665
- Fielding EJ, Lundgren PR, Taymaz T, Yolsal ÇS, Owen SE (2013) Fault-slip source models for the 2011 M7.1. Van earthquake in Turkey from SAR interferometry, pixel offset tracking, GPS and seismic waveform analysis. *Seismol Res Lett* 84(4):1–15
- Gogus OH, Pysklywec RN (2008) Mantle lithosphere delamination driving plateau and synconvergent extension in eastern Anatolia. *Geology* 36:723–726
- Gök R, Pasyanos ME, Zor E (2007) Lithospheric structure of the continent-continent collision zone: eastern Turkey. *Geophys J Int* 169:1079–1088
- Görür N, Çagatay MN, Zabcı C, Sakiç M, Akkök R, Şile H, Örcen S (2015) The Late Quaternary tectono-stratigraphic evolution of the Lake Van, Turkey. *Bull Min Res Exp* 151:1–46
- Gürbüz A, Gürer OF (2008) Tectonic geomorphology of the north Anatolian Fault zone in the Lake Sapanca Basin (eastern Marmara Region, Turkey). *Geosci J* 12(3):215–225
- Hall R (1976) Ophiolite emplacement and the evolution of the Tau-rus suture Zone, south-eastern Turkey. *Geol Soc Am Bull* 87:1078–1088
- Kaden H, Peeters F, Lorke A, Kipfer R, Tomonaga Y, Karabiyikoglu M (2010) Impact of lake level change on deep-water renewal and oxic conditions in deep saline Lake Van, Turkey. *Water Res Res* 46:W11508
- Kempe S, Khoo F, Degens ET (1978) Hydrography of Lake Van and its drainage area. In: Degens ET, Kurtman F (eds) *Geology of Lake Van*, vol 169. MTA press, New York, pp 30–44
- Kipfer R, Aeschbach-Hertig W, Baur H, Hofer M, Imboden DM, Signer P (1994) Injection of mantle type helium into Lake Van (Turkey): the clue for quantifying deep water renewal. *Earth Planet Sci Lett* 125:357–370
- Kocuyigit A (2013) New field and seismic data about the intraplate strike-slip deformation in Van region, East Anatolian plateau, E. Turkey. *J Asian Earth Sci* 62:586–605
- KOERI (Kandilli Observatory and Earthquake Research Institute) (2011) Van Earthquake (Mw 7.2) Evaluation Report as of 27 October 2011. Bogazici University, Istanbul, p 3
- Kuzucuoglu C, Christol A, Mouralis D, Dogu AF, Akkopru E, Fort M, Brunstein D, Zorer H, Fontugne M, Karabiyikoglu M, Scaillet S, Reys JL, Guillou H (2010) Formation of the upper pleistocene terraces of Lake Van. *J Quat Sci* 25:1124–1137
- Lahn E (1948) Türkiye Göllerinin Jeolojisi ve Jeomorfolojisi Hakkında Bir Etüt. MTA press, Ankara, p 87
- Landmann G, Reimer A, Lemcke G, Kempe S (1996) Dating Late Glacial abrupt climate changes in the 14,570 year long continuous varve record of Lake Van, Turkey. *Palaeogeogr Palaeoclimatol Palaeoecol* 122:107–118
- Litt T, Anselmetti FS (2014) Lake Van drilling project PALEOVAN. *Quat Sci Rev* 104:1–7
- Litt T, Krastel S, Sturm M, Kipfer R, Orcen S, Heumann G, Franz SO, Ulgen UB, Niessen F (2009) ‘PALEOVAN’, International Continental Scientific Drilling Program (ICDP): site survey results and perspectives. *Quat Sci Rev* 28:1555–1567
- Macdonald R, Sumita M, Schmincke HU, Baginski B, White JC, Ilnicki SS (2015) Peralkaline felsic magmatism at the Nemrut volcano, Turkey: impact of volcanism on the evolution of Lake Van (Anatolia) IV. *Contrib Mineral Petrol* 169:34
- Manga M, Brodsky EE (2006) Seismic triggering of eruptions in the far field: volcanoes and geysers. *Annu Rev Earth Planet Sci* 34:263–291
- Pinar A, Honkura Y, Kuge K, Matsushima M, Sezgin N, Yilmazer M, Ögtücü Z (2007) Source mechanism of the 2000 November 15 Lake Van earthquake (Mw = 5.6) in eastern Turkey and its seismotectonic implications. *Geophys J Int* 170(2):749–763
- Rasas FM, Duarte JC, Terrinha P, Valadares V, Matias L (2009) Morphotectonic characterization of major bathymetric lineaments in Gulf of Cadiz (Africa-Iberia plate boundary): Insights from analogue modelling experiments. *Mar Geol* 261:33–47
- Reilinger R, McClusky S, Vernant P, Lawrence S, Ergintay S, Cakmak R et al (2006) GPS constraints on continental deformation in the Africa-Arabia-Eurasia continental collision zone and implications for the dynamics of plate interactions. *J Geophys Res* 111:B05411
- Reimer A, Landmann G, Kempe S (2008) Lake Van, eastern Anatolia, hydrochemistry and history. *Aquat Geochem* 15(1–2):195–222
- Schmincke HU, Sumita M, Paleovan scientific team (2014) Impact of volcanism on the evolution of Lake Van (eastern Anatolia) III: periodic (Nemrut) vs. episodic (Süphan) explosive eruptions and climate forcing reflected in a tephra gap between ca. 14 ka and ca. 30 ka. *J Volcanol Geotherm Res* 285:195–213
- Şengör AMC, Kidd WSF (1979) The post-collisional tectonics of the Turkish-Iranian Plateau and a comparison with Tibet. *Tectonophysics* 55:361–376

- Şengor AMC, Özeren S, Zor E, Genc T (2003) East Anatolian high plateau as a mantle-supported, N-S shortened domal structure. *Geophys Res Lett* 30(24):8045
- Stockhecke M, Sturm M, Brunner I, Schmincke HU, Sumita M, Kipfer R, Cukur D, Kwiecien O, Anselmetti FS (2014) Sedimentary evolution and environmental history of Lake Van (Turkey) over the past 600,000 years. *Sedimentology* 61(6):1830–1861
- Sumita M, Schmincke HU (2013) Impact of volcanism on the evolution of Lake Van II: temporal evolution of explosive volcanism of Nemrut Volcano (eastern Anatolia) during the past ca. 0.4 Ma. *J Volcanol Geotherm Res* 253:15–34. doi:[10.1016/j.jvolgeores.2012.12.009](https://doi.org/10.1016/j.jvolgeores.2012.12.009)
- Taskin B, Sezen A, Tugsal UM, Erken A (2013) The aftermath of 2011 Van earthquakes: evaluation of strong motion, geotechnical and structural issues. *Bull Earthq Eng* 11(1):285–312
- Toker M (2013) Time-dependent analysis of aftershock events and structural impacts on intraplate crustal seismicity of the Van earthquake (Mw 7.1, 23 October 2011), E-Anatolia. *Cent Eur J Geosci* 5(3):423–434
- Tomonaga Y, Brennwald MS, Kipfer R (2011) Spatial distribution and flux of terrigenous He dissolved in the sediment pore water of Lake Van (Turkey). *Geochim Cosmochim Acta* 75(10):2848–2864
- Tomonaga Y, Brennwald MS, Meydan AF, Kipfer R (2014) Noble gases in the sediments of Lake Van – solute transport and palaeoenvironmental reconstruction. *Quat Sci Rev* 104:117–126
- Utkucu M (2013) 23 October 2011 Van, Eastern Anatolia, earthquake (M W 7.1) and seismotectonics of Lake Van area. *J Seismol* 17:783–805
- Wong HK, Finckh P (1978) Shallow structures in Lake Van. In: Degens ET, Kurtman F (eds) *Geology of Lake Van*, vol 169. MTA press, New York, pp 20–28